



Wideband and low dispersion slow light in slotted photonic crystal waveguide

Jun Wu, Yanping Li^{*}, Chao Peng, Ziyu Wang

State Key Laboratory of Advanced Optical Communication Systems and Networks, School of Electronics Engineering and Computer Science, Peking University, Beijing, 100871, China

ARTICLE INFO

Article history:

Received 10 February 2010
Received in revised form 16 March 2010
Accepted 16 March 2010

Keywords:

Photonic crystal waveguide
Slow light
Dispersion

ABSTRACT

We present a procedure to generate wideband and low dispersion slow light in slotted photonic crystal waveguide. By shifting the first and second rows of air holes of slotted photonic crystal waveguide, the bandwidth of slow light can be increased, with small group velocity dispersion. Using 2D plane wave expansion method, we numerically demonstrate slow light with the nearly constant group indices of 23, 42, and 54 over 17.6 nm, 6.7 nm and 3.3 nm bandwidth, respectively. The maximal normalized delay-bandwidth product is 0.26. From the fabrication's point of view, shifting the position of holes is easier to be controlled technically than changing the diameters of air holes. In addition, our simulations suggest this design is tolerant to deviation for positions of the first two rows of air holes. Therefore, the proposed approach decreases the dependence on the fabrication accuracy.

© 2010 Elsevier B.V. All rights reserved.

1. Introduction

Photonic crystal waveguide (PhCW) guides light due to the defect state in photonic band gap (PBG) [1,2], which generates the slow light phenomena near the photonic band edge because of structure dispersion [3–6]. Slow light offers the possibility for spatial compression of optical energy and the enhancement of linear and nonlinear optical effects [7–11]. Unfortunately, slow light usually accompanies with large group velocity dispersion (GVD), which distorts the pulse shape and damages the signals in high bit rate.

It is useful to generate the slow light over a wide bandwidth. One of the main criteria for slow light device property is the normalized delay-bandwidth product $n_g(\Delta\omega/\omega)$, which is proportional to the delay-bandwidth product per unit length. Wideband and low dispersion slow light in conventional PhCW has been achieved by tailoring the parameters, such as chirping photonic crystal coupled waveguide [12], tuning the waveguide width [13,14], perturbing the radius of air holes adjacent to the waveguide [5,15], shifting the first and second rows of air holes adjacent to the waveguide in the direction perpendicular to the waveguide [16], and shifting the third row of air holes in the direction parallel to the waveguide [11]. Moreover, the technique based on liquid infiltration of PhCW waveguide can generate dispersion free slow light [17].

In conventional PhCW, light is usually strongly confined in the high-index guiding layer, which may counteract the interaction between light and low index materials. Slotted waveguide was first presented by Almeida et al. [18], which can confine light in a narrow slot in which is filled with low-refractive index material. Recent researches indicate that

the slotted PhCW can combine the ability to confine light in air with the dispersion control available from PhCW [19]. Furthermore, the intrinsic physical properties of silicon make it difficult to be used for active optical devices. In slotted waveguide structure, nonlinear or electro-optical (EO) material can be filled into the slot region, which allows combining the high nonlinearity and the fast EO characteristics of polymer with strong light confinement in low index material. It makes the slot waveguide an attractive technology for optical sensors [20–22]. This structure can be used to realize low-threshold all-optical logical switch, compact logical device, optical tweezing, and EO material-based active optical devices [23,24]. Slow light phenomenon with group index in excess of 100 and light localization are also obtained in such a structure [25,26].

In this paper, inspired by Ref. [16], we design a procedure to generate wideband and low dispersion slow light in slotted PhCW by shifting the first and second rows of air holes in the direction normal to the line waveguide. The dependences of dispersion property on the position of the first two rows will be investigated. Then for the optimized structures, the group indices and the corresponding normalized delay-bandwidth products will be calculated. Finally, the tolerance to deviation for positions of air holes caused by fabrication errors will also be discussed.

2. Design and modeling

The slotted PhCW is formed by replacing a row of air holes with a narrow air slot in photonic crystal, as shown in Fig. 1. In the slotted PhCW, the effective index in the waveguide is lower than that in the surrounding slab. Therefore, the dispersion curve of the guided mode has positive slope [27]. Moreover, in the slotted PhCW, the guided modes are slotted modes, whose dispersion curves are pushed up due to the presence of air slot, and interact with higher frequency bands to

^{*} Corresponding author.

E-mail address: liyip@pku.edu.cn (Y. Li).

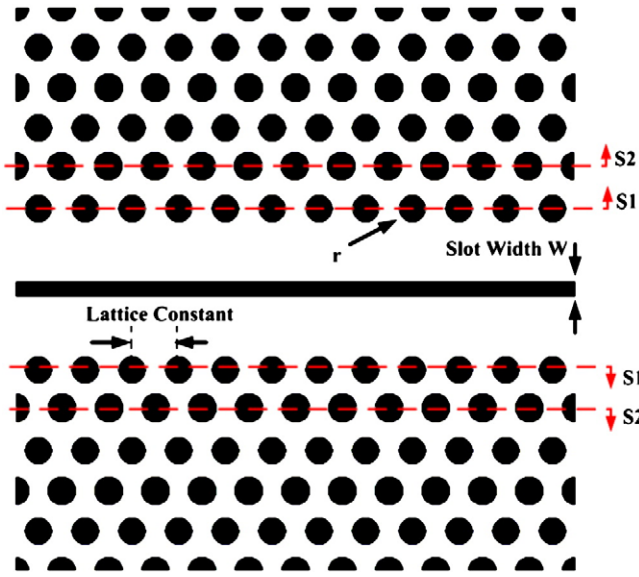


Fig. 1. Structure model of slotted PhCW: s_1 and s_2 (dashed lines) describe the shift from the ideal lattice of the first and second rows symmetrically in the direction perpendicular to waveguide. The shifts towards the outside are positive.

change their dispersion properties. In contrast, in the conventional PhCW, the guided modes change their dispersion properties due to the interaction with lower bands.

The modification of the radii and positions of the air holes in first two rows are two of the widely used methods for improving the properties of the guided modes. Li et al. [16] and Baba et al. [11] indicated that shifting the air holes was relatively easier to be controlled than changing their radius, from the aspect of fabrication processes. Therefore, changing the position of the first two rows of holes could be a promising approach to optimize the dispersion properties.

In the following discussions, we define parameters s_1 and s_2 to describe the deviation of first and second rows from the ideal lattice in the direction perpendicular to the waveguide, marked with dashed lines in Fig. 1, and the shifts towards the outside are positive.

As a reference, we first perform the calculation for dispersion properties of standard slotted PhCW without shifting the air holes. We assume the lattice constant $a = 430$ nm, the radius of air hole $r = 0.34a$, the slot width $w = 0.31a$, and the thickness of the slab $h = 210$ nm. Here we employ the 2D plane wave expansion (PWE) method with effective index of the slab of 2.9 to analyze the dispersion behavior. In Fig. 2(a) the dispersion curves for TE polarized light-wave are shown, the solid line indicates the defect guided mode, and the slab mode region is lined out in gray. It is found that the slotted PhCW supports one mode in the PBG. The group velocity v_g of the PBG mode can be obtained from the slope of the dispersion curve, i.e., $v_g = \frac{d\omega}{dk} = \frac{c}{n_g}$, where ω is the frequency, k is the wavevector in the propagation direction, and n_g is the group index. The GVD parameter β_2 is given by the second order derivative of the dispersion relation as

$$\beta_2 = \frac{d^2k}{d\omega^2} = \frac{1}{c} \frac{dn_g}{d\omega}$$

The group index n_g and GVD parameter β_2 are plotted as the function of wavelength λ in Fig. 2(b). It is found that the n_g varies rapidly with wavelength in the slow light region. Correspondingly, the parameter β_2 increases drastically in this region, on the order of magnitude of 10^{-21} s²/m.

The guided modes in the PhCW can be understood as a mixture of “index guided” mode and “gap guided” mode, which can be categorized

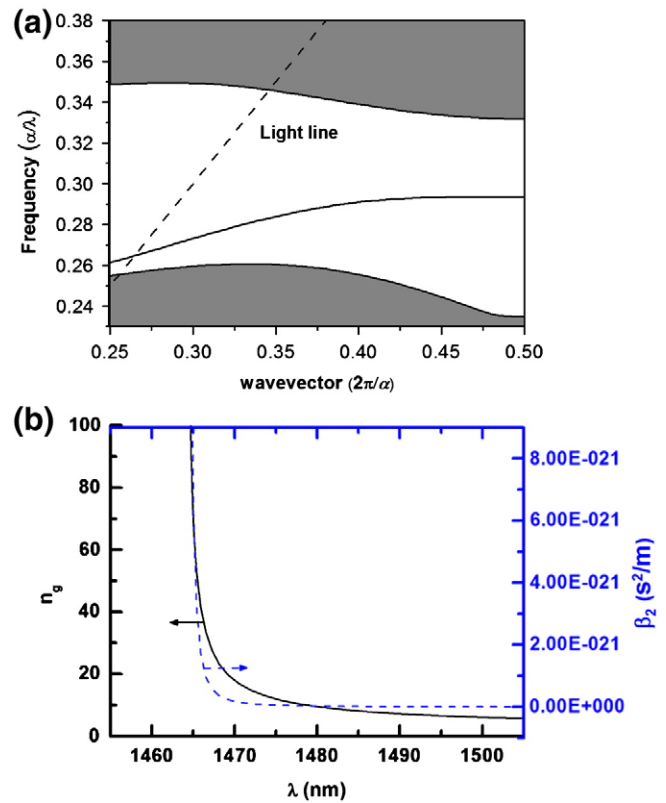


Fig. 2. (a) Calculated dispersion curve of standard slotted PhCW, where $a = 430$ nm, $r = 0.34a$, and $w = 0.31a$. The horizontal and the vertical axis indicate the wavevector in the propagation direction and the normalized frequency a/λ , respectively. The solid line indicates defect mode, and the gray regions represent slab mode. (b) Group index n_g and the GVD parameter β_2 as the function of wavelength λ for the defect guided mode plotted in (a).

with respect to their field distributions [5]. In the small wavevector region, the guided mode has its field concentrated inside the waveguide core, and the mode profile is similar to that of fundamental mode in a ridge waveguide. The dispersion curve is linear, which corresponds to the small n_g . Hence, in this region, the mode is usually referred to be “index guided” mode. In the large wavevector region, the guided mode penetrates into photonic crystal lattice, and the slope decreases several orders of magnitude, which corresponds to extremely larger n_g . Thus, the guided mode in such region is “gap guided” mode.

Firstly, we exploit the dispersion characteristics of slotted PhCW by shifting the first and second rows of air holes adjacent to the waveguide in the direction perpendicular to the waveguide. The parameters s_1 and s_2 vary in a certain region, while other structure parameters are identical with the standard slotted PhCW. The calculation results are illustrated in Fig. 3.

From panel (a) of Fig. 3, it is clearly noticed that when s_1 increases from $-0.02a$ to $0.03a$, the whole dispersion curves shift towards the lower frequency and the slope decreases. The reason of the frequency shifting can be understood from the electromagnetic variation theorem [1]: enlarging the high refractive index region would lead to lower mode frequency that minimizes the energy of the mode. However, it is also found that the normalized delay-bandwidth product is still extremely small in these cases, when merely s_1 is shifted.

On the other hand, panel (b) of Fig. 3 shows an interesting phenomenon by shifting the second row of air holes. When s_2 increase from $-0.15a$ to $0.10a$, the whole dispersion curves shift towards the lower frequency, as explained by the electromagnetic variation theorem. In contrast, as the s_2 further increases to $0.15a$, the dispersion curve shifts towards the higher frequency in the small wavevector region, since the slope of the curve decreases more rapidly to counteract

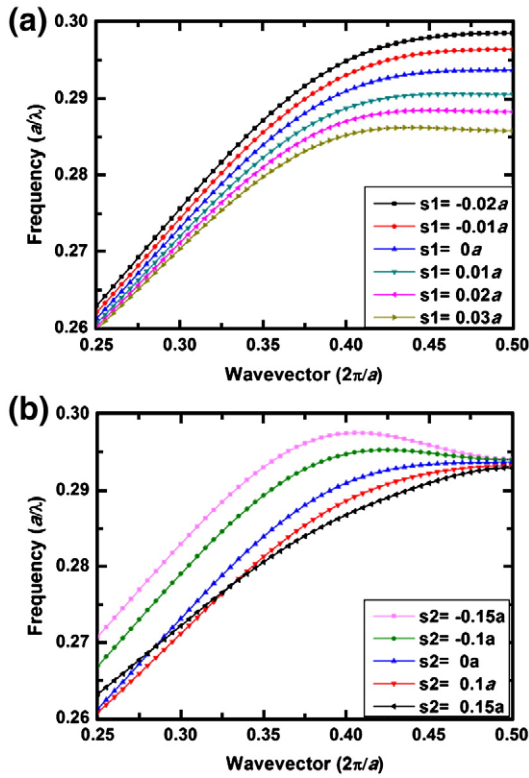


Fig. 3. (a) Dispersion curves for different shift of the first row from $s_1 = -0.02a$ to $s_1 = 0.03a$ with $s_2 = 0$. (b) Dispersion curves for different shift of the second row from $s_2 = -0.15a$ to $s_2 = 0.15a$ with $s_1 = 0$.

the normal frequency shifting. As a result, a reversed frequency shifting is presented in such region.

The phenomenon that increasing s_1 or s_2 would cause the decrease in the slope of the dispersion curve can be qualitatively understood by coupled-mode theory [28]. Taking the case of 1D Bragg grating as an example, the coupling between forward and backward propagating modes generates photonic PBG, and the width of the gap is determined by the coupling strength. Similarly, the coupling between the contra-directional propagating modes produces the gap in PhCW. As we discussed above, the modes in the PhCW are the mixture of “index guided” mode and “gap guided” mode. Particularly, they refer to “index guided” mode at the small k region and the fields concentrate in waveguide core. The increasing of s_1 or s_2 would lead to the increase of the high refractive index region. As a result, the coupling strength increases between waveguide defect mode and low energy photonic crystal modes, since the low energy modes are more likely concentrated in the high refractive index region. For the similar reason, the coupling strength decreases between waveguide mode and high energy photonic crystal modes. Therefore, at the small k region, the slope of the curve decreases and the band moves to higher frequency.

Our optimization goal is to obtain the slow light with large n_g and small β_2 in a wide wavelength region, corresponding to the large normalized delay-bandwidth product. This can be achieved by combining the effects of shifting the two rows of air holes. By properly increasing s_2 , the slope decreases at the small k region because of the reverse trends discussed above. This corresponds to larger n_g in such region. The flat dispersion curve can thus be obtained in relatively larger bandwidth. Then, adjusting s_1 finely, the increase of s_1 will further enlarge n_g in the whole region, while it increases more rapidly at the large k region. In this case, shifting s_1 and s_2 simultaneously would lead to a large and constant n_g over wide bandwidth. Therefore, we get the desired slow light with large normalized delay-bandwidth product.

Fig. 4(a) illustrates the calculated dispersion curves for three examples of optimized slotted PhCW, where the guided mode in the

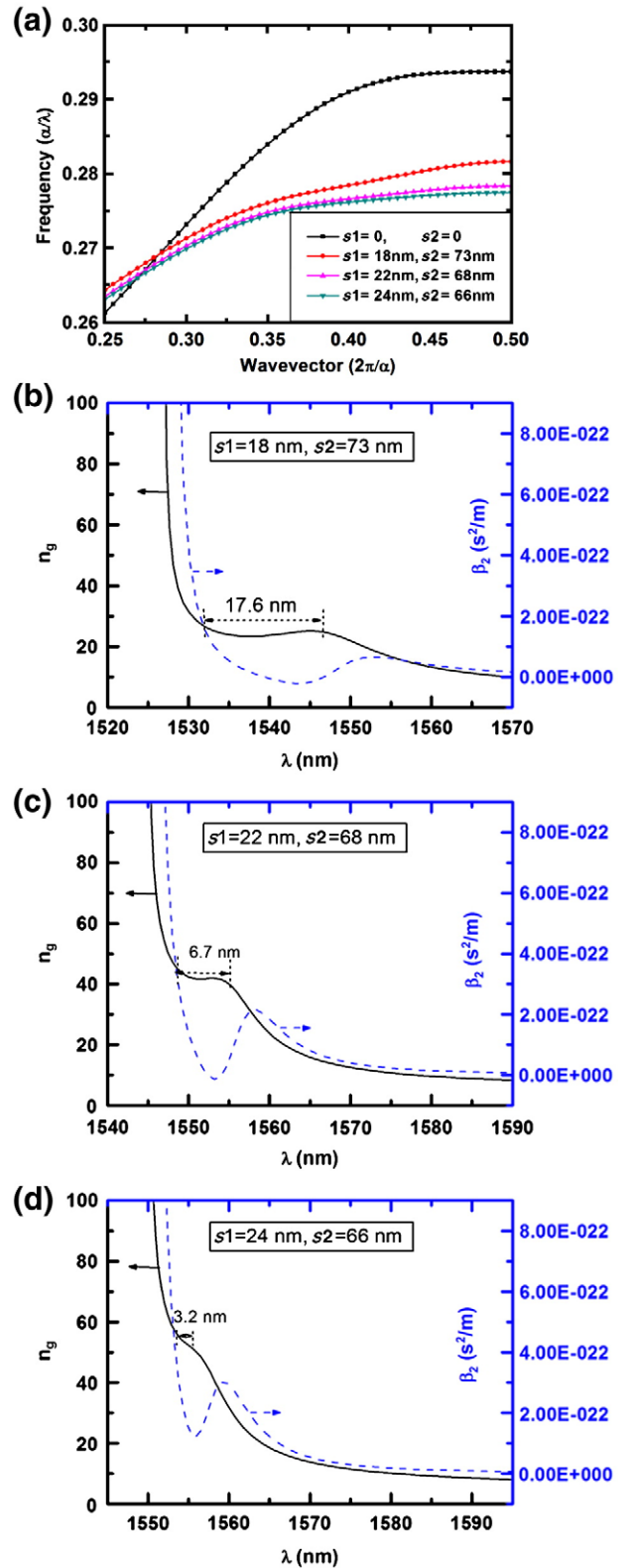


Fig. 4. (a) Calculated dispersion curves for optimized slotted PhCW, where the guided mode in the standard slotted PhCW is also plotted with black line as a reference. The corresponding group index n_g and the GVD parameter β_2 are plotted as a function of wavelength λ for the cases with ($s_1 = 18$ nm, $s_2 = 73$ nm), ($s_1 = 22$ nm, $s_2 = 68$ nm), and ($s_1 = 24$ nm, $s_2 = 66$ nm) in the panels (b), (c), and (d), respectively.

standard slotted PhCW is also plotted with black line as a reference. The first row of air holes shifts towards the outside 18 nm, 22 nm, and 24 nm, while the second row of air holes shifts towards the outside

73 nm, 68 nm, and 66 nm, respectively. Fig. 4(b)–(d) illustrate the corresponding n_g and β_2 characteristics as the function of wavelength λ . As seen in Fig. 4(b), the n_g is quasi-constant and equal to 23 between 1535 nm and 1550 nm. The bandwidth $\Delta\lambda = 17.6$ nm, which is calculated by considering n_g within $\pm 10\%$, and the normalized delay-bandwidth product is 0.26. The group index plateaus lead to negligibly small β_2 on the order of magnitude of 10^{-22} s²/m, which is one order of magnitude lower than the standard slotted PhCW in Fig. 2(b). From the cases in Fig. 4(c), (d), it can be found that the further increments of s_1 make n_g enhance to 38 and 54, nevertheless, the bandwidth $\Delta\lambda$ and the normalized delay-bandwidth product decrease, as summarized in Table 1. Even though there exists no flat band when n_g is over 10 in the standard slotted PhCW, for comparison with the optimized cases, the bandwidth and normalized delay-bandwidth product in the standard slotted PhCW at $n_g = 23$ are also shown in Table 1. These results indicate that shifting the first and second rows of air holes of slotted PhCW, wide band slow light can be obtained, with small GVD. In addition, the percentages of overlap between light and the slot are calculated. It is found that the percentage of overlap decreases for larger n_g , since the slotted mode penetrates into the photonic crystal lattice.

In the following, we discuss several advantages of the approach that shifting the first and second rows of air holes in slotted PhCW to obtain wide band slow light. Shifting the air holes is easier to be controlled in fabrication process when comparing with some other methods, such as changing the radius of the holes. Furthermore, the large normalized delay-bandwidth product can be achieved by utilizing the reversed trends of shifting two rows. It provides a recipe for designing procedure that the effects of shifting s_1 and s_2 can be investigated respectively, and then combined together. Moreover, the proposed approach has good tolerance to the deviation of shifting during fabrication, which can be illustrated by the following result.

In Fig. 4(c), we have got the optimized result as $s_1 = 22$ nm, $s_2 = 68$ nm, with n_g is 42, $\Delta\lambda$ is 6.7 nm, and normalized delay-bandwidth product is 0.18. Assuming there is ± 2 nm deviation of shifting based on this case. As shown in Fig. 5(a), n_g is almost a constant at the wavelength 1552 nm, although the dispersion curve shape changes with the deviation. Moreover, we can see from Fig. 5(b) that, for the wavelength from 1548 nm to 1555 nm, the β_2 for three cases vary in a small range. Furthermore, the normalized delay-bandwidth products are 0.14 and 0.21 for $s_2 = 66$ nm, $s_2 = 70$ nm, respectively, without severely performance degradation. This shows that the tiny deviation for positions of the first two rows of the air holes has little effect on the optimized results. Therefore, it is acceptable for the fabrication precision in the 2 nm scale. It will reduce the accuracy requirement in fabrication process.

3. Conclusion

In summary, wideband and low dispersion slow light has been obtained in slotted photonic crystal waveguide by shifting the first and second rows of air holes. We numerically demonstrate that this scheme can tailor the dispersion relation to get the almost constant n_g

Table 1

Bandwidth $\Delta\lambda$, group index n_g , the GVD parameter β_2 , the normalized delay-bandwidth product $n_g(\Delta\omega/\omega)$, and the percentage of overlap between light and the slot for standard and optimized slotted PhCW.

Adjusted parameter s_1 (nm)	s_2 (nm)	$\Delta\lambda$ ($\pm 10\%$, nm)	n_g	Order of magnitude of β_2 (s ² /m)	n_g ($\Delta\omega/\omega$)	Overlap
0	0	1.2	23	10^{-21}	0.01	10.40%
18	73	17.6	23	10^{-22}	0.26	10.00%
22	68	6.7	42	10^{-22}	0.18	9.71%
24	66	3.3	54	10^{-22}	0.11	9.53%

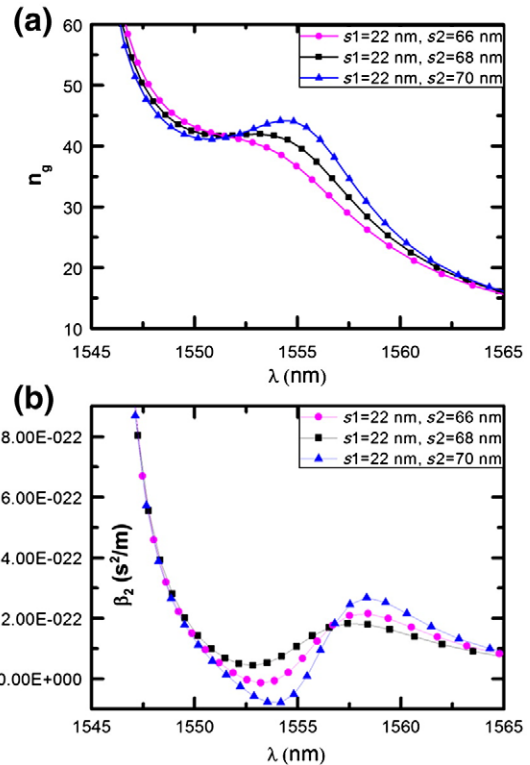


Fig. 5. (a) The group index n_g as the function of wavelength λ for different shift of the second row from $s_2 = 66$ nm to $s_2 = 70$ nm with $s_1 = 22$ nm. (b) The GVD parameter β_2 as the function of wavelength λ .

with substantial bandwidth, and the normalized delay-bandwidth product increases enormously. We demonstrate slow light with the nearly constant group indices of 23, 42, and 54 over 17.6 nm, 6.7 nm and 3.3 nm bandwidth, respectively. The corresponding normalized delay-bandwidth products are 0.26, 0.18, and 0.11. In addition, we show that shifting the air holes is tolerant to deviation, and it is easier to be controlled from the aspect of fabrication process comparing with changing the diameters of air holes. Therefore, it relaxes the constriction on the fabrication accuracy.

Acknowledgments

The authors are grateful to Professor T. Baba, Professor A. Yu. Petrov and Doctor A. Di Falco for useful discussions. This work is supported by the National Basic Research Programme of China under Grant No 2006CB604901, the National Natural Science Foundation of China under Grant No 60807016, and the Doctoral Fund of Ministry of Education of China under Grant No 200800011003.

References

- [1] J.D. Joannopoulos, R.D. Meade, J.N. Winn, Photonic Crystals: Molding the Flow of Light, Princeton University Press, Princeton, 1995.
- [2] S.G. Johnson, S. Fan, P.R. Villeneuve, J.D. Joannopoulos, L.A. Kolodziejski, Phys. Rev. B 60 (1999) 5751.
- [3] Y.A. Vlasov, M. O'Boyle, H.F. Hamann, S.J. Mcnab, Nature 438 (2005) 65.
- [4] T. Kawasaki, D. Mori, T. Baba, Fourth IEEE International Conference on Group IV Photonics, 2007, p. 143.
- [5] L.H. Frandsen, A.V. Lavrinenko, J. Fage-Pedersen, P.I. Borel, Opt. Express 14 (2006) 9444.
- [6] A. Säynätjoki, M. Mulot, J. Ahopelto, H. Lipsane, Opt. Express 15 (2007) 8323.
- [7] C. Monat, B. Corcoran, M. Ebnali-Heidari, C. Grillet, B.J. Eggleton, T.P. White, L. O'Faolain, T.F. Krauss, Opt. Express 17 (2009) 2944.
- [8] A. Baron, A. Rytasnyanskiy, N. Dubreuil, P. Delaye, Q.V. Tran, S. Combrié, A. de Rossi, R. Frey, G. Roosen, Opt. Express 17 (2009) 552.
- [9] K. Inoue, H. Oda, N. Ikeda, K. Asakawa, Opt. Express 17 (2009) 7206.
- [10] B. Corcoran, C. Monat, C. Grillet, D.J. Moss, B.J. Eggleton, T.P. White, L. O'Faolain, T.F. Krauss, Nat. Photonics 3 (2009) 206.

- [11] Y. Hamachi, S. Kubo, T. Baba, *Opt. Lett.* 34 (2009) 1072.
- [12] D. Mori, T. Baba, *Opt. Express* 13 (2005) 9398.
- [13] A. Sakai, I. Katoh, D. Mori, T. Baba, Y. Takiguchi, *Proc. IEEE/LEOS Annual Meet.* 2004, ThQ5.
- [14] A.Yu. Petrov, M. Eich, *Appl. Phys. Lett.* 85 (2004) 4866.
- [15] S. Kubo, D. Mori, T. Baba, *Opt. Lett.* 32 (2007) 2981.
- [16] J. Li, T.P. White, L. O' Faolain, A. Giglesias-Iglesias, T.F. Krauss, *Opt. Express* 16 (2008) 6227.
- [17] M. Ebnali-Heidari, C. Grillet, C. Monat, B.J. Eggleton, *Opt. Express* 17 (2009) 1628.
- [18] V.R. Almeida, Q. Xu, C.A. Barrios, M. Lipson, *Opt. Lett.* 29 (2004) 1209.
- [19] A. Di Falco, L. O'Faolain, T.F. Krauss, *Photonics Nanostruct. Fundam. Appl.* 6 (2008) 38.
- [20] C.A. Barrios, M.J. Bañuls, V. González-Pedro, K.B. Gylfason, B. Sánchez, A. Griol, A. Maquieira, H. Sohlström, M. Holgado, R. Casquel, *Opt. Lett.* 33 (2008) 708.
- [21] H. Sun, A. Chen, L.R. Dalton, *IEEE Photon. J.* 1 (2009) 48.
- [22] A. Di Falco, L. O'Faolain, T.F. Krauss, *Appl. Phys. Lett.* 94 (2009) 063503.
- [23] J.M. Brosi, C. Koos, L.C. Andreani, M. Waldow, J. Leuthold, W. Freude, *Opt. Express* 16 (2008) 4177.
- [24] J.H. Wülbern, J. Hampe, A. Petrov, M. Eich, J.D. Luo, A.K.-Y. Jen, A. Di Falco, T.F. Krauss, J. Bruns, *Appl. Phys. Lett.* 94 (2009) 241107.
- [25] A. Di Falco, L. O'Faolain, T.F. Krauss, *Appl. Phys. Lett.* 92 (2008) 083501.
- [26] J. Wu, C. Peng, Y. Li, Z. Wang, *Chin. Phys. Lett.* 26 (2009) 014209.
- [27] S.G. Johnson, P.R. Villeneuve, S. Fan, J.D. Joannopoulos, *Phys. Rev. B.* 62 (2000) 8212.
- [28] O. Khayam, H. Benisty, *Opt. Express* 17 (2009) 14634.